SUBGLACIAL WATER LAYER AND GROUNDING LINE DERIVED FROM BACKSCATTERING COEFFICIENTS OF RADIO ECHO SOUNDING IN THE SHIRASE GLACIER AND ROI BAUDOUIN ICE SHELF, EAST ANTARCTICA

Fumihiko Nishio[1] and Seiho Uratsuka[2]

[1]*National Institute of Polar Research, 9–10, Kaga 1-chome, Itabashi-ku, Tokyo 173*
[2]*Communications Research Laboratory, 2–1, Nukui-Kitamachi 4-chome, Koganei 184*

Abstract: In the 1986–87 austral summer, ice thickness measurements using a new designed airborne radio echo sounding system were carried out in the Shirase Glacier drainage basin and Roi Baudouin Ice Shelf, Princess Ragnhild Coast, East Antarctica.

The accurate determination of ice thickness during the flight was supported by measurements of surface elevation calibrated over the open sea at the beginning and end of each flight with radar altimetry. Location was determined by an OMEGA system and satellite Global Positioning System (GPS).

The ice sheet profile along the flow line of the Shirase Glacier and ice shelf along the flight line from Asuka Camp to the Roi Baudouin Ice Shelf were determined and bottom features such as subglacier water layer and grounding line were clarified by finding the radio backscattering coefficients.

The accurate surface elevation and backscattering coefficients obtained from the radar equation are adequate for locating the grounding line and detecting its accurate location within a few kilometers.

It is also shown that the subglacial water layer was inferred from the backscattering coefficients of radio echo sounding along the Shirase Glacier flow line. The water layer thickness is estimated to be 0–30 cm at the interface between the base of the ice sheet and the bedrock in the regions downstream of Shirase Glacier.

1. Introduction

In the Japanese Antarctic Research Expedition (JARE) program, radio echo sounding has been conducted; a newly designed radio echo sounding system to be carried on a Pilatus PC-6 aircraft was developed in 1985 (Uratsuka *et al.*, 1988). In the 1986–87 austral summer, measurements of ice thickness using the new radio echo sounder were carried out in the Shirase Glacier drainage basin and the Roi Baudouin Ice Shelf, Princess Ragnhild Coast, East Antarctica (Fig. 1).

Measurements of ice sheet movements indicated thinning of the ice sheet in the Shirase Glacier drainage area (Nishio *et al.*, 1989; Naruse, 1979). The thinning could be caused by basal sliding if the base of the ice sheet is at the melting point (Mae and Naruse, 1978). Therefore, we measured the more detailed profile of ice thickness
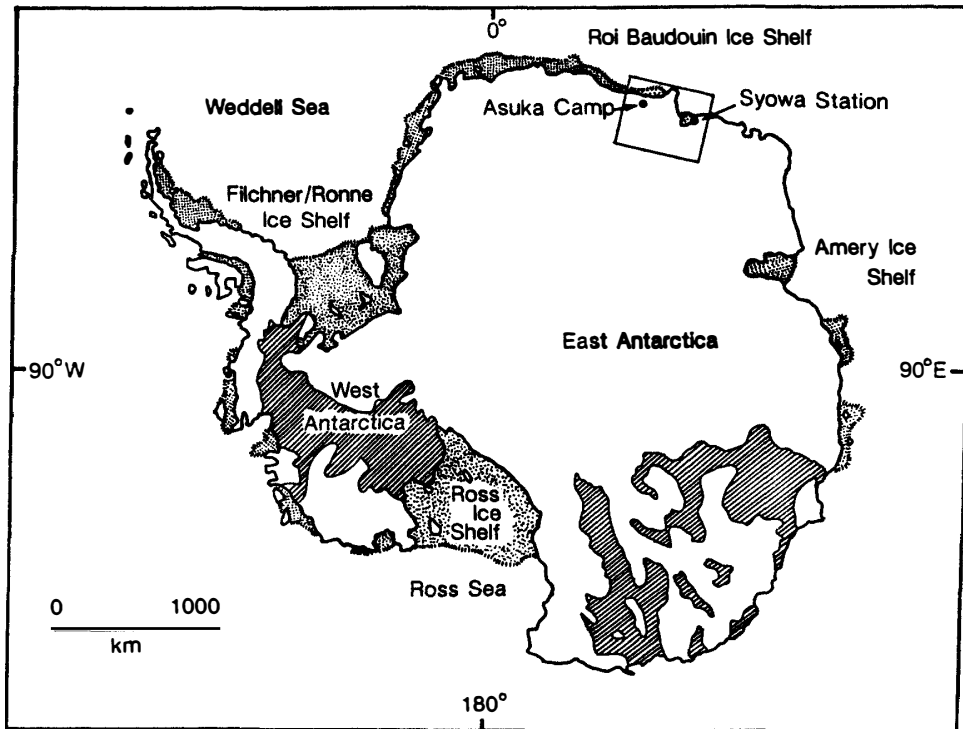
Fig. 1. Antarctica. The area of this study is outlined (Asuka Camp and Syowa Station). The floating ice shelves are shaded and the hachured regions are marine-based portions of the ice sheet resting on bedrock more than 500 m below sea level.
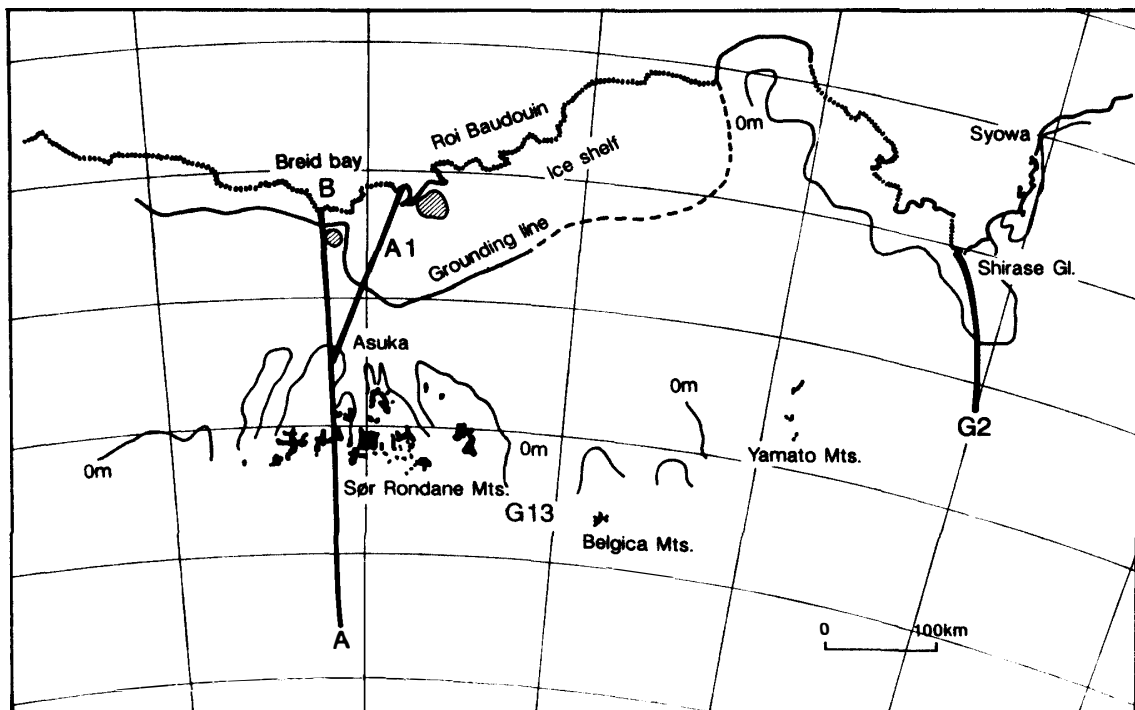

Fig. 2. Map of bedrock topography in the areas of Shirase Glacier, Yamato, Belgica and Sør Rondane Mountains. The only 0-m contour is depicted and grounding line of the Roi Baudouin Ice Shelf is shown by the solid line (the dotted line is infered). Straight thick solid lines show the flight course of ice thickness measurements by airborne radio echo sounding.

along the flow line of Shirase Glacier by radio echo sounding as shown in Fig. 2 and estimated the physical characteristics of the interface between the base of the ice sheet and the bedrock derived from radio backscattering coefficients calculated from the radar equation.

The Roi Baudouin Ice Shelf with a area of about 30000 km² is located north of the Sør Rondane Mountains and Belgica Mountains, downstream from the East Queen Maud Land ice sheet (Fig. 2). The surface elevation exhibits almost flat shape from the coastal edge of the ice shelf to the inland region and then it shows an abrupt steepening until the inland ice area (NISHIO et al., 1984).

So far, the ice thickness in this region has been determined by gravity measurements along a few surveyed lines from Breid Bay to the polar plateau through the Sør Rondane Mountains (VAN AUTENBOER and DECLEIR, 1978). A few profiles of gravity measurements showed that most of the base of ice sheet lies well below sea level and is grounded, but the grounding lines between Roi Baudouin Ice Shelf and the grounded ice sheet have not yet been determined by the gravity measurements.

The marine-based ice sheet in the northern part of the Sør Rondane Mountains and Belgica Mountains is drained by a series of outlet glaciers. In order to predict likely ice sheet and ice shelf responses to future change in climate, it is essential to determine the locations of grounding lines. It could be that the retreat of grounding lines is caused by net thinning of the ice shelf and, on the contrary, the grounding lines advance when the ice shelf and ice sheet are growing thicker. Therefore, it is important to determine the locations of grounding lines accurately.

This paper shows that the accurate surface elevation and radio backscattering coefficients obtained by radio echo sounding are useful for determining the locations of grounding lines and the physical conditions of the interface between ice sheet and bedrock.

2. Airborne Radio Echo Sounding Equipment and Data Recording

New airborne radio echo sounding (NIPR-III) equipment was designed prior to JARE 27 and used for the majority of this work.

The radio echo sounding system with 179 MHz was carried on a Pilatus PC-6 aircraft. The antenna array consisted of two (transmission and reception) antennas, 3 elements Yagi antenna of a quarter-wavelength, mounted beneath aircraft wings. The system was usually employed with a 250 ns nominally square pulse and a peak output power of 1 kW. Other pulse lengths of 60 ns and 1 μs could also be selected for sounding thinner or thicker ice. Each pulse was transmitted every 1 ms through a 3 element Yagi antenna; the received signals were amplified through a preamplifier of limiting low noise. The system performance with a 250 ns pulse at 1 kW power output was measured to be —110 dBm as the minimum sensitivity of the received signal.

The output signals from the receiver in A-scope form were provided to a digitizer for the recording system. Digitized signals of A-scope form, averaged over 256 frames where one frame is formed from the return signal from one pulse. The digitized signals are recorded every second by a 1/4-inch cartridge type digital data recorder through a data processor with the navigation data being altitude (radio and barometric altimeters

with thermometer), positioning (VLF/omega and GPS receiver), and attitude (Gyro).

3. Radio Backscattering Coefficients Derived from the Radar Equation

The radio backscattering coefficients of ice and bedrock interface are derived from the radar equation. The attenuation in ice and refraction effect air/ice interface should be taken into consideration to construct radar equation. The received signal from ice/bedrock interface is in the followings:

$$P_r = \frac{P_t G^2 \lambda^2 h \Gamma^2 \sigma_R^{\theta_2}(\theta_2) f^2(\theta_1) \cos^3 \theta_1}{2^6 \pi^2 H^3 L^2 \left(1 + \frac{z}{nH\xi}\right)\left(1 + \frac{z}{nH\xi^3}\right)^2 \xi^2} \; e^{-2\frac{\kappa z}{\xi \cos \theta_1}} \tag{1}$$

where P_t is the transmitted power, P_r the received power, G the antenna peak gain, λ the wave length in free space ($=1.67$ m), h the pulse length in free space, Γ and $\sigma_R^{\theta_2}$ are the transmission rate at the air/ice interface and the scattering coefficients at the ice sheet bottom, $f(\theta_1)$ the normalized antenna pattern, $\alpha = 4.343 \times \kappa$ the attenuation coefficient, n the refractive index, H the airplane altitude, z the ice thickness which can be calculated from the time difference between two peaks and L the system loss. ξ defined as $\xi = \cos \theta_2/\cos \theta_1$, θ_2 is the refractive angle (equal to the incidence angle to the bottom) and is related to θ_1 through Snell's law.

In addition, these parameters can be calculated from the delay time t using the following relation.

$$\frac{H}{\cos \theta_1} + \frac{nz}{\cos \theta_2} = \frac{ct}{2} \tag{2}$$

In this paper the radio backscattering coefficient is defined as $\Gamma^2 \sigma_R^{\theta_2}$ for convenience because of difficulty of separation between Γ and $\sigma_R^{\theta_2}$.

4. Estimation of Subglacial Water Layer

The power reflection coefficients obtained by ground-based radio echo sounding along the flow line of the Shirase Glacier indicated that the areas where the ice sheet has been thinning and where high driving stress has been shown in the Shirase Glacier area correspond to areas with a "wet" bed and "water-film" bed (Ohmae et al., 1988).

To clarify the bottom features of ice sheet based on the radio scattering characteristics, we have calculated the radio backscattering coefficients at 179 MHz and 0°C for several types of boundaries taking the following values of permittivity for polar ice, various waters, and a representative rock as tabulated in Table 1 (Shabtaie et al., 1987). In order to estimate the subglacial water layer, radio backscattering coefficients are deriv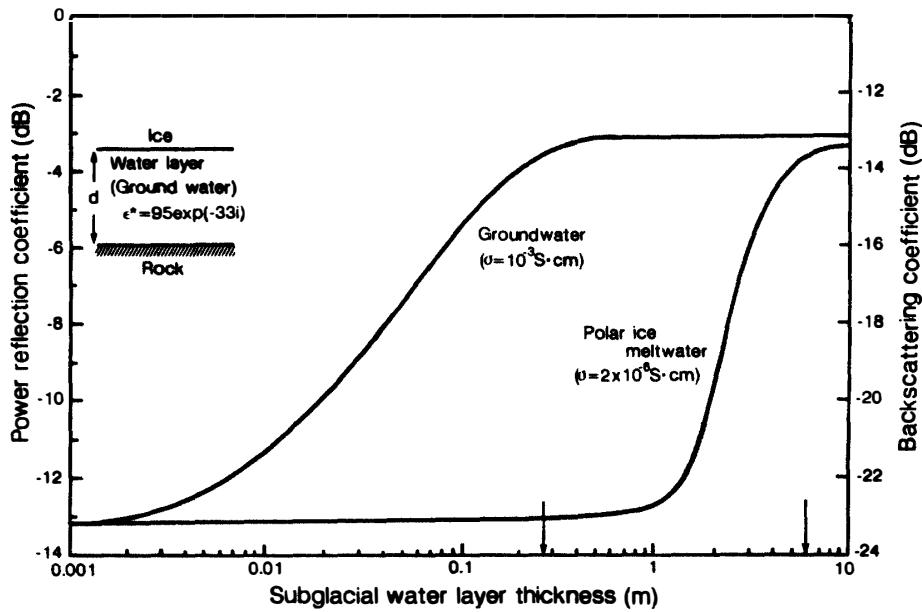ed from the reflection coefficient calculated using a three layer model. Figure 3 shows the power reflection coefficient and backscattering coefficient as a function of the thickness of the subglacial water layer for two ice-water-rock models, one with groundwater ($\sigma = 10^{-3}$ S·cm) and the other with polar ice meltwater ($\sigma = 2 \times 10^{-6}$ S·cm). The values of backscattering coefficient was -8 to -10 dBm underneath the ice shelf corresponding to the ice/seawater interface as shown in

Table 1.   Values of permittivity for polar ice, water and rock
(SHABTAIE et al., 1987).

Ice	$\varepsilon^* = 3.2 \exp(-0.007\,i)$
Seawater (salinity—32‰)	$\varepsilon^* = 1500 \exp(-87\,i)$
Groundwater (salinity—1‰)	$\varepsilon^* = 95 \exp(-33\,i)$
Polar ice meltwater	$\varepsilon^* = 86 \exp(-0.07\,i)$
Rock	$\varepsilon^* = 7.4 \exp(-22\,i)$

Fig. 3.   Power reflection coefficient (SHABTAIE et al., 1987) and backscattering coefficient as a function of the thickness of the subglacial water layer for two ice-water-rock models, one with groundwater ($\sigma = 10^{-3}\,S \cdot cm$) and the other with polar ice meltwater ($\sigma = 2 \times 10^{-6}\,S \cdot cm$).

Fig. 6.

From this diagram the thickness of subglacial water layer at the base of the Shirase Glacier is estimated as shown in Fig. 8.

5.   Grounding Lines

Because of the importance of the grounding line to arguments relating to the stability of marine ice sheets and to measurements aimed at discovering whether the marine-based ice sheet is growing or shrinking, we have made a particular effort to describe where it lies along the coastline of the Roi Baudouin Ice Shelf.   To find the grounding lines, we now consider all the elevation data obtained by airborne radio-echo sounding.   Since the ice surface elevations measured from the radar altimeter are tied to the sea surface, the elevation contour map can be used to interpolate the grounding line between known points.   For a floating ice shelf in hydrostatic equilibrium,

$$\bar{\rho} \cdot D = \rho_w (D - H) \tag{3}$$

where D is the ice thickness, H the elevation of the ice shelf above sea level, ρ_w the density of the displaced seawater and $\bar{\rho}$ the mean density of the ice column. On the Roi Baudouin Ice Shelf, ρ will generally will vary from place to place, but the average density is assumed to be 900 kg/m³. The density of seawater is taken to be 1027.5 g/m³ as reported by SHABTAIE and BENTLEY (1987). Therefore, the resulting hydrostatic equation is $H=0.1241$ D(m).

6. Results and Discussion

Figure 4 shows the profile of the ice sheet surface, bedrock elevation and radio backscattering coefficients along flight line AB between Breid Bay and the polar plateau through the Asuka Camp and Sør Rondane Mountains in Fig. 2. The surface elevation gradually increases toward the Sør Rondane Mountains from Breid Bay where the ice rise is formed and most of the base of ice sheet lies below sea level at a depth of approximately 400 m, that is, it is a marine-based ice sheet which is grounded on the bedrock.

In contrast, the ice sheet on the southern side of the Sør Rondane Mountains with surface elevation of more than 2500 m has a damming effect on the ice flow caused by the elevated surface elevation, and the bedrock elevation on the polar plateau is higher than 1000 m, extending to the Valkyrdomen in the central region of Queen Maud Land ice sheet (DREWRY, 1983). The radio backscattering coefficients reflected at the ice/bedrock interface in the marine-based ice sheet are a little larger by approximately 10–20 dB than those on the polar plateau. We can interpret the substantially larger power reflection coefficients and also the larger radio backscattering coefficients in the marine-based ice sheet as indicating the presence of subglacial water at the ice/bedrock interface or a wet base in the bottom layer of the ice sheet.
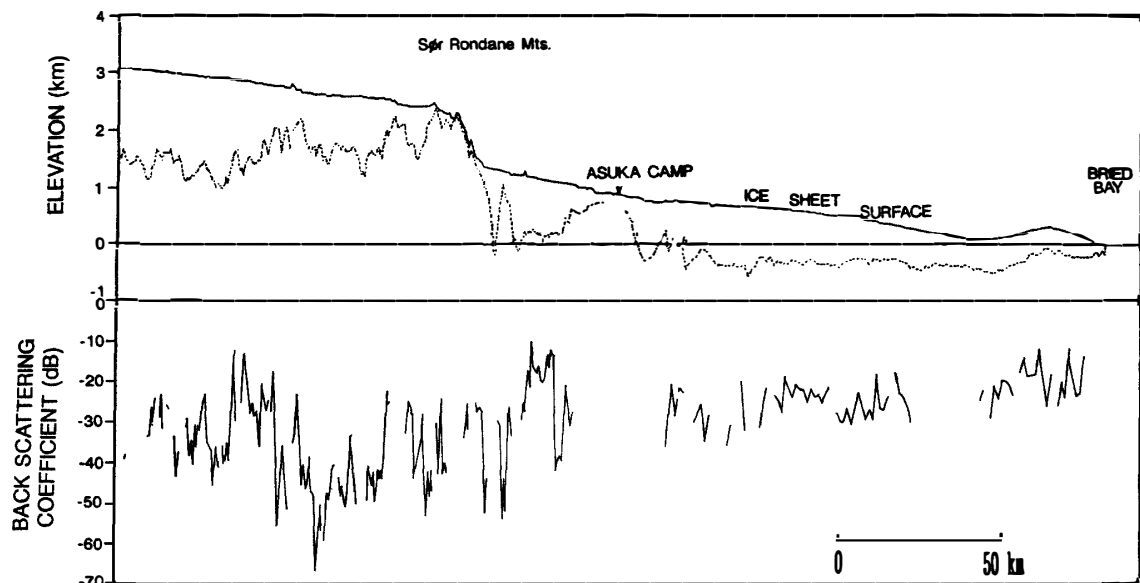

Fig. 4. Profile of ice sheet surface, bedrock elevation and backscattering coefficients along the flight line between Breid Bay and the interior region on the ice sheet through Asuka Camp shown by the solid line AB in Fig. 2.

In Fig. 5, the profile of ice sheet surface, bedrock elevation and bottom topography of Roi Baudouin Ice Shelf are shown along flight line A1 between Asuka Camp and the coastal edge of the ice shelf in Fig. 2.   The white line in Fig. 5 indicates the flight altitude of aircraft at approximately 400 m during the radio echo sounding.   The echo strength at the ice/seawater interface in the ice shelf is stronger than that at the ice/bedrock interface underneath the ice sheet.   The coastal region in the ice shelf shows smoother bottom features than those near the grounding line; the bottom crevasse appears to be at the bottom of the ice shelf.

Figure 6 shows the profile of ice sheet surface, bedrock elevation and bottom topography of the ice shelf, and radio backscattering coefficients obtained by the digitized data in Fig. 5.   The elevation of the ice shelf bottom calculated by hydrostatic equilibrium eq. (3) using the value of ice thickness is in good agreement with the measured ice shelf bottom indicated by the dotted line in Fig. 6, but the computed elevation of ice sheet bottom is far from the measured elevation of bedrock under the grounded ice sheet beyond the grounding line.   Therefore, it becomes possible to find the accurate location of the ice shelf grounding line in the area where surface elevation increases toward the interior region.   The radio backscattering coefficients also indicate rapid decrease at the grounding line toward the interior region.   These coefficients in the grounding zone tend to be weaker by approximately 20 dB than those in the floating ice shelf downstream from the grounding line.   We can also interpret the larger value of approximately 20 dB of radio backscattering coefficients at the ice/seawater interface than at the ice/rock interface.   To define the value of radio backscattering coefficient at the ice/seawater interface in Fig. 6, it is determined by the average value of -8 dB to -10 dB.   Based on the average value, the diagram shown in Fig. 3 is computed by a conversion procedure from the power reflection coefficient as a function of the thickness of the subglacial water layer described by SHABTAIE et al. (1987).

Thus, the accurate surface elevation, the ice thickness measurement and the radio backscattering coefficients obtained by the radar equation can predict the accurate location of the grounding line, probably within a few kilometers.

In the Shirase Glacier drainage area, the area with surface elevation of about 2500 m has a wet bed as has been derived from the power reflection coefficient in the wet model (OHMAE et al., 1988).   This area agrees with the area where the bed temperature is above $-1°C$, thinning of the ice sheet has been occurring and there is a high driving stress.

The profile of ice sheet surface and bedrock elevation along the flow line of Shirase Glacier from the terminus to G2 is shown in Fig. 7.   The terminus of Shirase Glacier is floating ice approximately 450 m thick.   The surface elevation rapidly increases toward the interior, but the bedrock elevation is nearly close to sea level.

In Fig. 7, there are bright (purple color) radar returns characteristic of wet conditions.   Our interpretation rests heavily on melting point temperatures calculated as a function of pressure by assuming a steady state.

In the area where the surface elevation is lower than 2000 m in the Shirase Glacier along the flow line between the terminus and G2, the radio backscattering coefficients are calculated using radar eq. (3) and the subglacial water layers are estimated using the diagram indicated in Fig. 3.   Where the Shirase Glacier rests on a wet bed, its
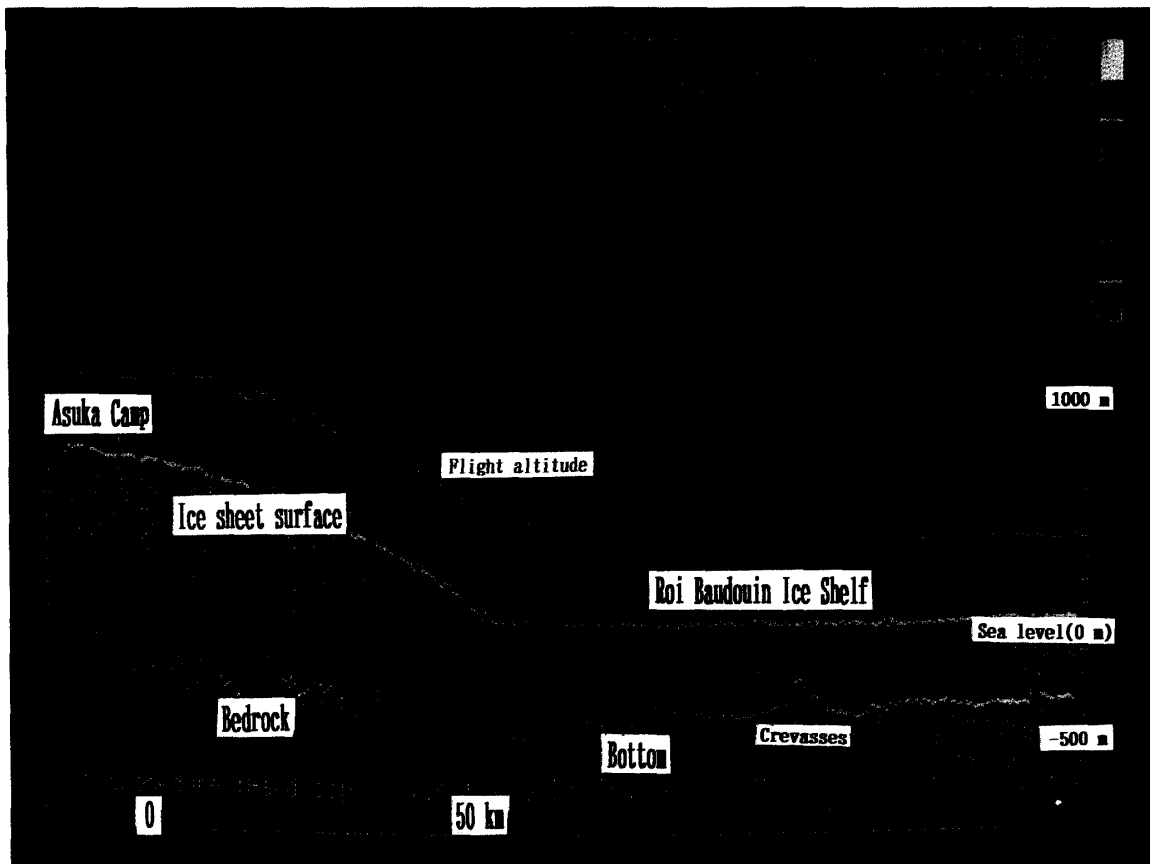
Fig. 5. Profile of ice sheet surface, bedrock elevation and bottom topography of Roi Baudouin Ice Shelf along flight line of A1 between Asuka Camp and the coastal edge of the ice shelf shown in Fig. 2.
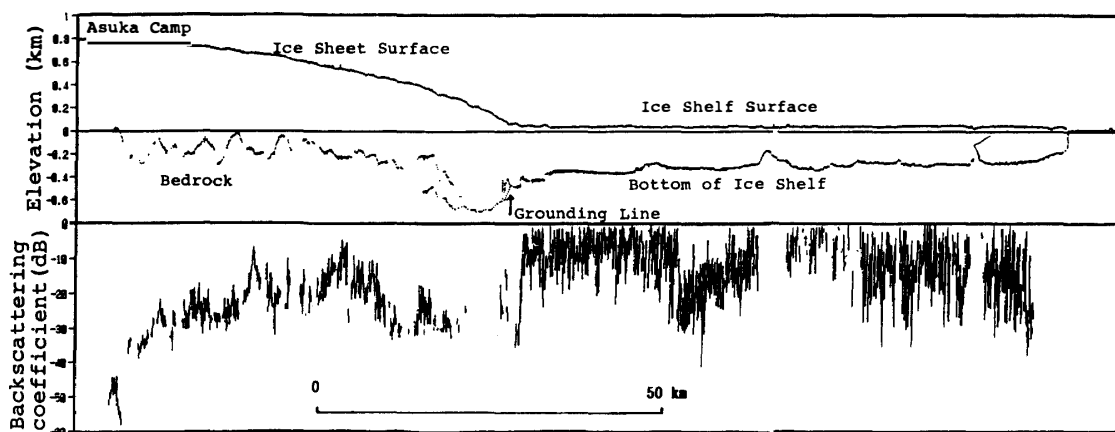

Fig. 6. Profile of ice sheet surface, bedrock elevation, backscattering coefficients and bottom topography of Roi Baudouin Ice Shelf along flight line A1 between Asuka Camp and the coastal edge of the ice shelf shown in Fig. 2.

weight is supported partly by the subglacial water and partly by the solid bed. As shown in Fig. 8, in the terminus of Shirase Glacier, sea water is present in the areas of floating ice and in the areas of surface elevation less than 1500 m, and the subglacial
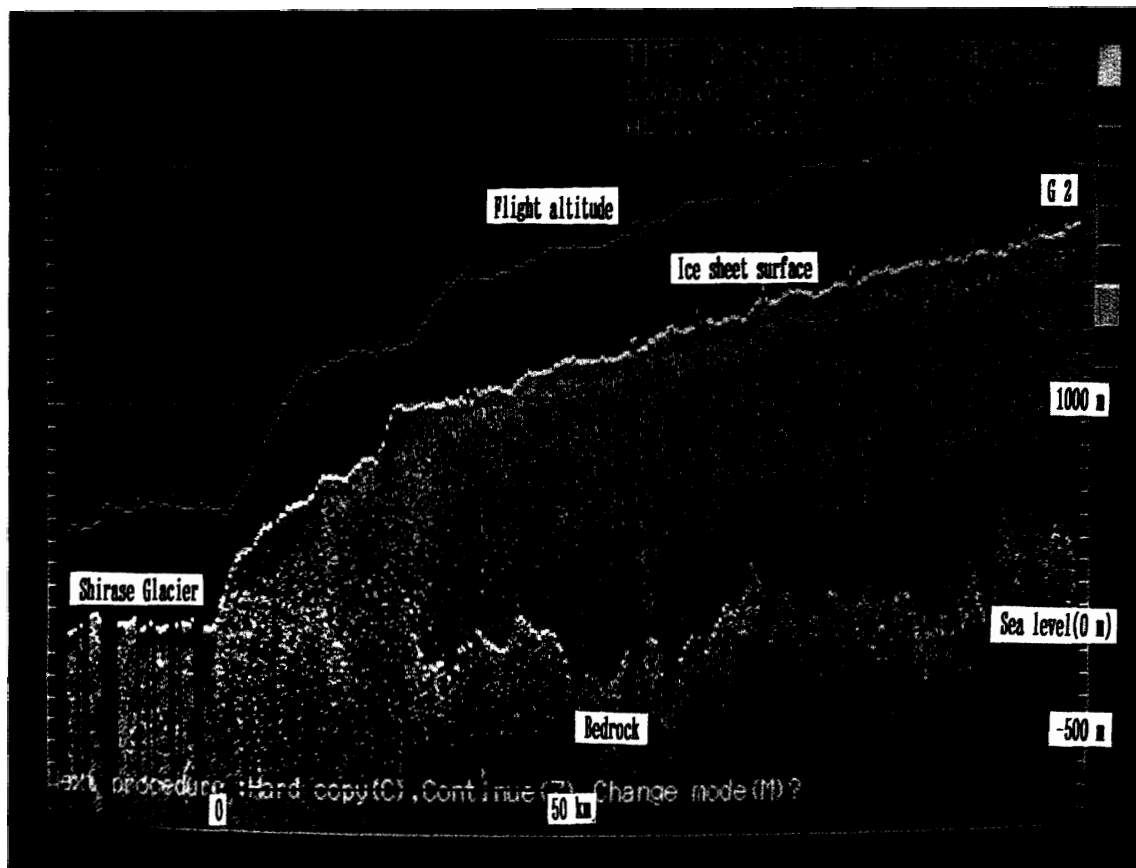
Fig. 7. Profile of ice sheet surface, bedrock elevation and bottom topography of ice sheet along the flow line of Shirase Glacier between G2 and Shirase Glacier shown in Fig. 2.
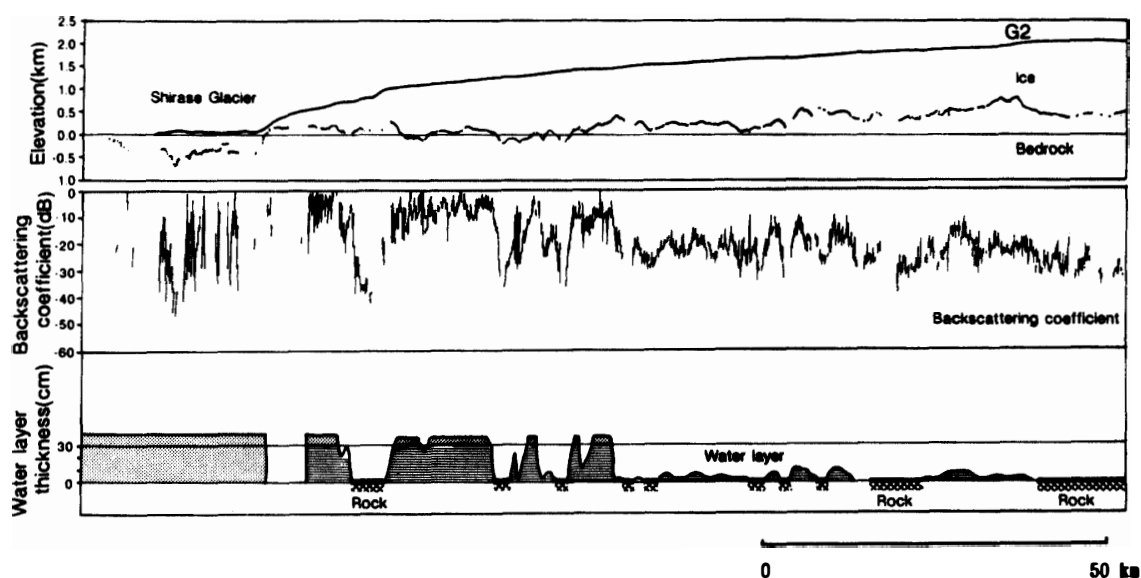

Fig. 8. Profile of ice sheet surface, bedrock elevation, backscattering coefficients and the estimated subglacial water layer at the base of the ice sheet along the flow line of Shirase Glacier between G2 and Shirase Glacier shown in Fig. 2.

water layer is thicker than 30 cm, but, in the areas of surface elevation more than 1500 m, it is thinner or the bed is wet in basal conditions.

The bed underneath the ice sheet at elevation less than 2000 m is not frozen everywhere. This area is in good agreement with that where the bed temperature is above −1°C calculated by steady state assumption, but it might be frozen to the solid bed beneath the ice sheet in the interior portions. This new radar sounding confirms that the bed in the lower portions of Shirase Glacier is also wet and that a subglacial water layer may be present where radar sounding suggests the exsistence of trapped water associated with the slopes of surface terraces in Fig. 8. For a more detailed interpretation of basal conditions in Shirase Glacier, we would require the surface topography by satellite altimetry, ice thickness measurements and continuous direct velocity measurements.

Acknowledgments

References

Dʀᴇᴡʀʏ, D. J. (1983): Antarctica; Glaciological and Geophysical Folio. Cambridge, Cook Hammond and Kell.

Mᴀᴇ, S. and Nᴀʀᴜsᴇ, R. (1978): Possible causes of ice sheet thinning in the Mizuho Plateau. Nature, **273**, 291–292.

Nᴀʀᴜsᴇ, R. (1979): Thinning of the ice sheet in Mizuho Plateau, East Antarctica. J. Glaciol., **24**, 45–52.

Nɪsʜɪo, F., Isʜɪᴋᴀᴡᴀ, M., Oʜᴍᴀᴇ, H., Tᴀᴋᴀʜᴀsʜɪ, S. and Kᴀᴛsᴜsʜɪᴍᴀ, T. (1984): A preliminary study of glacial geomorphology in area between Breid Bay and the Sør Rondane Mountains in Queen Maud Land, East Antarctica. Nankyoku Shiryô (Antarct. Rec.), **83**, 11–28.

Nɪsʜɪo, F., Mᴀᴇ, S., Oʜᴍᴀᴇ, H., Tᴀᴋᴀʜᴀsʜɪ, S., Nᴀᴋᴀᴡᴏ, M. and Kᴀᴡᴀᴅᴀ, K. (1989): Dynamical behavior of the ice sheet in Mizuho Plateau, East Antarctica. Proc. NIPR Symp. Polar Meteorol. Glaciol., **2**, 97–104.

Oʜᴍᴀᴇ, H., Nɪsʜɪo, F. and Uʀᴀᴛsᴜᴋᴀ, S. (1988): Distribution of reflected power from the bed by radio echo-sounding in Shirase glacier drainage area, East Dronning Maud Land, Antarctica. Ann. Glaciol., **12**, 124–126.

Sʜᴀʙᴛᴀɪᴇ, S. and Bᴇɴᴛʟᴇʏ, R. C. (1987): West Antarctic ice streams draining into the Ross ice shelf; Configuration and mass balance. J. Geophys. Res., **92**, B2, 1311–1336.

Sʜᴀʙᴛᴀɪᴇ, S., Wʜɪʟʟᴀɴs, I. M. and Cʜᴀʀʟᴇs, R. B. (1987): The Morphology of ice streams A, B, and C, West Antarctica, and their environs. J. Geophys. Res., **92**, B9, 8865–8883.

Uʀᴀᴛsᴜᴋᴀ, S., Nɪsʜɪo, F., Oʜᴍᴀᴇ, H. and Mᴀᴇ, S. (1988): Inference of radio scattering parameters of Antarctic ice sheet using 179 MHz airborne radio echo sounding data. Proc. 1988 International Geoscience and Remote Sensing Symposium (IGARSS '88) ESA SP-284, Edinburgh, UK, 157–160.

Vᴀɴ Aᴜᴛᴇɴʙᴏᴇʀ, T. and Dᴇᴄʟᴇɪʀ, H. (1978): Glacier discharge in the Sør Rondane, a contribution to the mass balance of Dronning Maud Land, Antarctica. J. Glaciol., **6**, 69–81.